Augmentor Wing Propulsive-Lift Concept Acoustic Characteristics

Michael D. Falarski*
NASA Ames Research Center and U.S. Army Air Mobility Research and Development Laboratory, Moffett Field, Calif.

John F. Wilby†
Bolt Beranek and Newman, Canoga Park, Calif.
and
Thomas N. Aiken‡
NASA Ames Research Center, Moffett Field, Calif.

A wind-tunnel investigation was conducted to determine the nature, strength, and variation with airspeed of the acoustic sources of the augmentor wing propulsive-lift concept. The augmentor wing overall noise is dominated by the high-frequency jet mixing noise characteristic of the lobed primary nozzle. The augmentor modifies the intensity and propagation characteristics of the jet sources, especially those that exist inside the augmentor. The interaction of the turbulent flow with the augmentor creates flow-frequency, low-intensity surface noise and trailing-edge noise. These sources dominate any jet mixing noise that is present at the low frequencies and could become significant if the jet noise were suppressed by treating the augmentor with a lining tuned to the jet noise source location. The far-field noise of the untreated augmentor is unaffected by airspeed; however, this may not be the case when the jet noise is suppressed, because the trailing-edge surface pressure and correlations with far-field noise do show a reduction with forward speed.

Nomenclature

c_f	=	flap chord, cm (in.)
c_n	=	primary nozzle spacing, cm (in.)
c_s	=	shroud chord, cm (in.)
f	=	frequency, Hz
h	=	primary nozzle height, cm (in.)
OASPL	=	overall sound pressure level, dB ref. 2×10^{-5} N/m^2 (0.0002 μbar)
P_a	=	atmospheric pressure, kg/m^2 (psia)
P_T	=	primary nozzle total pressure, kg/m^2 (psia)
P_T/P_a	=	primary nozzle pressure ratio
SPL	=	sound pressure level, dB ref. 2×10^{-5} N/m^2 (0.0002 μbar)
V_{jet}	=	primary nozzle isentropic jet velocity, m/sec (fps)
V_∞	=	freestream velocity, m/sec (fps)
y	=	spanwise station with respect to trailing edge, cm (in.) (see Fig. 3)
x	=	chordwise station with respect to trailing edge, cm (in.) (see Fig. 3)
z	=	distance downstream of nozzle exit plane, cm (in.) (see Fig. 3)
α	=	angle of attack with respect to wing chord, deg
δ_f	=	flap angle, deg (see Fig. 3)
θ	=	acoustic angle with respect to jet axis, deg
ρ	=	correlation coefficient
τ	=	delay time, msec
τ_m	=	delay time for maximum correlation, msec

Received Jan. 16, 1976; presented as Paper 76-79 at the AIAA 14th Aerospace Sciences Meeting, Washington, D.C., Jan. 26-28, 1976; revision received May 3, 1976.
Index category: Aircraft Noise, Powerplant.
*Aerospace Engineer. Member AIAA.
†Research Scientist.
‡Aerospace Engineer.

Introduction

The augmentor wing is one of several propulsive-lift concepts being investigated for application to commercial, turbofan-powered, STOL aircraft. In this concept, a wing trailing-edge ejector system is used to augment the high-pressure fan bypass air. Because commercial STOL aircraft will be operated out of airports nearer densely populated areas than commercial CTOL aircraft, the STOL aircraft will have to be significantly quieter.

Experimental investigations have shown that, by combining a lobed primary nozzle, to enhance the turbulent jet mixing, and an augmentor acoustic lining, to absorb the jet mixing noise, a substantial reduction in augmentor noise can be achieved. Further reduction of the noise requires a more complete understanding of the nature and strength of all of the acoustic sources; these may include augmentor surface turbulence noise, augmentor trailing-edge noise, and turbulent mixing noise inside and downstream of the augmentor.

This paper presents the results of a wind-tunnel investigation of the characteristics of the augmentor acoustic sources, especially those generated by the interaction of the turbulent flow with the augmentor surfaces and edges. The experiments were conducted in the NASA Ames 7- × 10-ft. wind tunnel using a quasi-two-dimensional model.

Model Description

The quasi-two-dimensional augmentor model had a 76-cm (30-in.) span, a constant airfoil section, and no sweep. The end-plate boundary-layer control used during the aerodynamic test was sealed for the acoustic experiment. For the static tests ($V\infty = 0$), the test section inlet was blocked to prevent tunnel recirculation, and the model was oriented with the jet parallel to the test section centerline. The walls of the test section were line with a 7.6-cm (3-in.) layer of acoustic foam. The far-field noise was measured by five 0.6-cm (0.25-in.) microphones equipped with nose cones (see Fig. 1). The model acoustic directivity was measured with a boom-

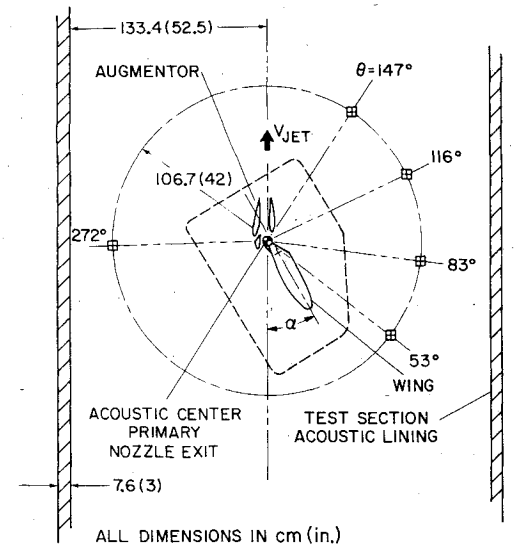

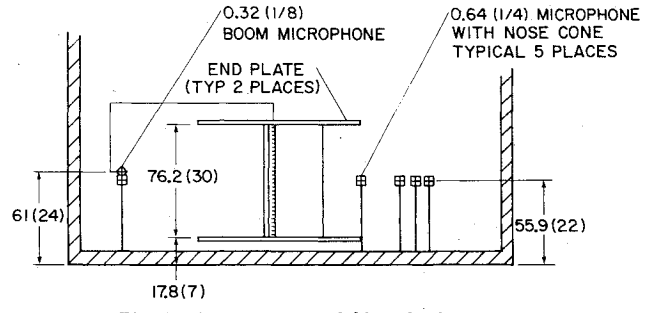

Fig. 1 Augmentor model installation details.

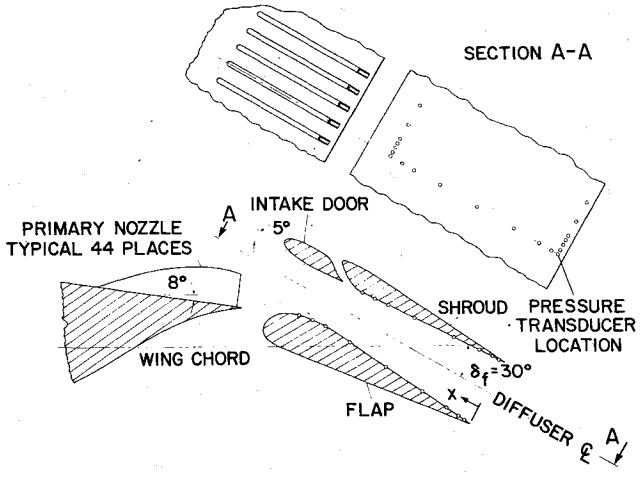

Fig. 2 Geometric details of augmentor and surface pressure transducer locations.

mounted 0.3-cm (0.125-in.) microphone. All microphones were located on a circle with a radius of 107 cm (42 in.); the center of the circle was at the lobed nozzle exit. The internal surface static pressure fluctuations were measured with 0.25-cm (0.10-in.) piezoelectric transducers installed flush with the flap and shroud internal surfaces at several spanwise and chordwise stations.

The augmentor model used for this investigation simulates a cruise-compatible concept. The ejector systems is designed to retract, leaving the lobed primary nozzle exposed to provide cruise propulsion (see Fig. 2). The augmentor consists of a 44-lobe primary nozzle, a flap, a shroud, and an intake door. The high-pressure primary air entrains ambient air into the augmentor from the wing upper surface, the slot between the flap and wing, and the slot between the intake door and

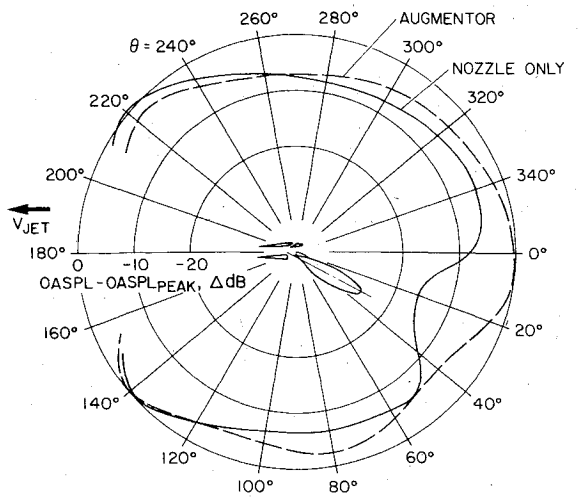

Fig. 3 Far-field acoustic directivity; $P_T/P_a = 2.09$.

shroud. The increase in overall system momentum afforded by the augmentor is indicated by the augmentation ratio, which is defined as the ratio of the total system thrust to the primary nozzle thrust. The augmentation ratio for the take-off configuration ($\delta_f = 30°$) was 1.30.

To verify that the augmentor aerodynamic characteristics were the same as those measured during an earlier investigation in which the augmentor geometry was optimized, the augmentor exit velocity distribution was measured at two spanwise locations. The augmentor demonstrated the same nonuniform exit distribution with primary flow attachment to the flap as previously measured.

Tests

To permit investigation of the primary nozzle far-field noise, the model was installed initially without the augmentor flap and shroud. The wing chord plane was set at $\alpha = -8°$ for the streamwise jet alignment. Acoustic directivity and fixed microphone signals were recorded over a primary pressure ratio (P_T/P_a) range of 1.27 to 2.63.

These tests were followed by installation of the augmentor at $\delta_f = 30°$. The angle of attack α of the model was decreased to $-30°$, and the fixed microphone and directivity measurements were repeated at the same pressure ratios. Surface transducers were installed and the pressure fluctuations recorded at various locations on the flap and shroud. The frequency spectra for both the microphones and transducers were computed on-line using a one-third-octave band real-time spectral analyzer.

A miniature accelerometer was used to measure the dynamic response of the flap and shroud structure to the turbulent flow at several spanwise and chordwise locations; frequency spectra of the accelerometer were compared with the surface pressure transducer output. The trailing-edge structure of both flap and shroud were stiffened to reduce interference of vibrations below 1000 Hz, to insure a sufficient signal-to-noise ratio.

Cross-correlations were performed between pairs of surface pressure transducers to investigate the propagation of surface turbulence and internal noise through the augmentor. The reference transducer was taken as the location nearest the leading edge of either the flap or shroud. Correlation measurements also were made between far-field microphones and pressure transducers to identify acoustic sources. In either case, the input signals first were filtered through phase-matched octave-band filters. The filtered signals were cross-correlated using a real-time correlation analyzer in clipped mode. The correlation operation was repeated three times to magnify the coefficient for octave-band center frequencies of 500, 1000, 2000, 4000, 8000, and 16,000 Hz. Correlation

measurements were made at a nozzle pressure ratio of 2.09. A small sample of data was subjected to narrow-band spectral analysis to insure the absence of supersonic shock-induced screech. All correlations were performed on-line to avoid any phasing errors inherent in dynamic data recording equipment.

To study the influence of forward speed, the model attitude was changed to $\alpha = 0°$ to insure proper augmentor inlet flow. The pressure transducers were located at the positions for which the highest correlations had been indicated previously. The far-field noise and surface pressure response was measured for freestream velocities (m/sec) of 0, 28, 40, 49 (0, 92, 130, 160 fps) at a pressure ratio of 2.09. Correlations between microphones and transducers were performed at $V_\infty = 0$ and 49 m/sec (0 and 160 fps).

Results

Augmentor Far-Field Acoustics

The acoustic directivity of the lobed nozzle alone is typical of a simple jet in that it is symmetric about the jet axis with the peak occurring at 135° (see Fig. 3). When the signal was filtered in octave bands, the symmetry remained, but the peak noise angle decreased with increasing frequency. The only deviation from the expected is forward at $\theta = 0°$ to 40° where the wing interferes with the noise propagation.

Installation of the augmentor produces a directivity pattern that is no longer symmetric about the jet axis, a result, perhaps, of the nonuniform augmentor jet. The peak noise under the wing occurred closer to the jet axis ($\theta = 140°$), and the angle for peak noise became essentially independent of frequency from $f = 1000$ to 16,000 Hz. A second noise peak under the wing can be seen in the augmentor directivity at about $\theta = 75°$. Spectral analysis shows that this peak is caused by a high-frequency source ($f > 16{,}000$ Hz).

Spectral analysis of the noise of the lobed nozzle alone shows the noise to be broadband, with the peak at a very high frequency (see Fig. 4). The spectral content is similar for $\theta = 116°$ and 83°. Addition of the augmentor increases the low-frequency noise. The peak at $f = 40{,}000$ Hz is still visible, along with a second lower-level peak at 12,500 Hz. The augmentor frequency spectra are not strong functions of acoustic angle except at points close to the jet axis ($\theta = 147°$).

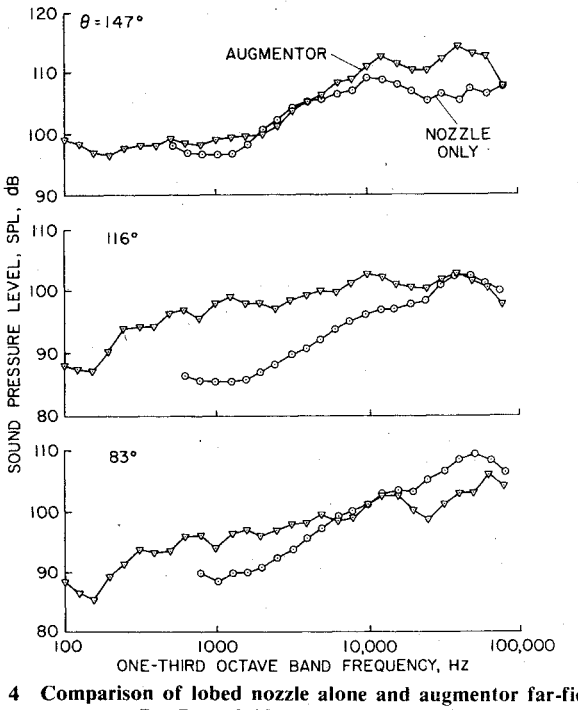

Fig. 4 Comparison of lobed nozzle alone and augmentor far-field frequency spectra; $P_T/P_a = 2.09$.

Spectral peaks with frequencies of 40,000, 12,500, and 630 Hz are visible at all angles.

A typical variation of augmentor spectra with primary nozzle pressure ratio is shown in Fig. 5. For $P_T/P_a \leq 2.09$ the spectra are similar. At higher pressure ratios, supersonic shock-induced screech contributes to the acoustic power at $f > 10{,}000$ Hz. For pressure ratio less than 2.09, the acoustic energy above $f = 4000$ Hz shows an eighth-power dependence on jet velocity, whereas at lower frequency this dependency reduces to the fifth or sixth power.

Augmentor Surface Pressure

The surface pressure spectra measured on the flap and shroud are broadband in character, with a broad spectral peak. The frequency of this peak increased with nozzle velocity and decreased as distance from the nozzle increased. At a given location, the spectra can be collapsed into a single curve if the frequency is nondimensionalized with respect to

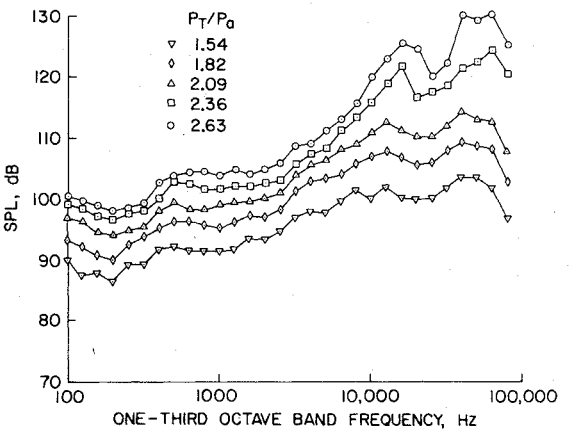

Fig. 5 Variation of augmentor far-field noise with pressure ratio: $\theta = 147°$.

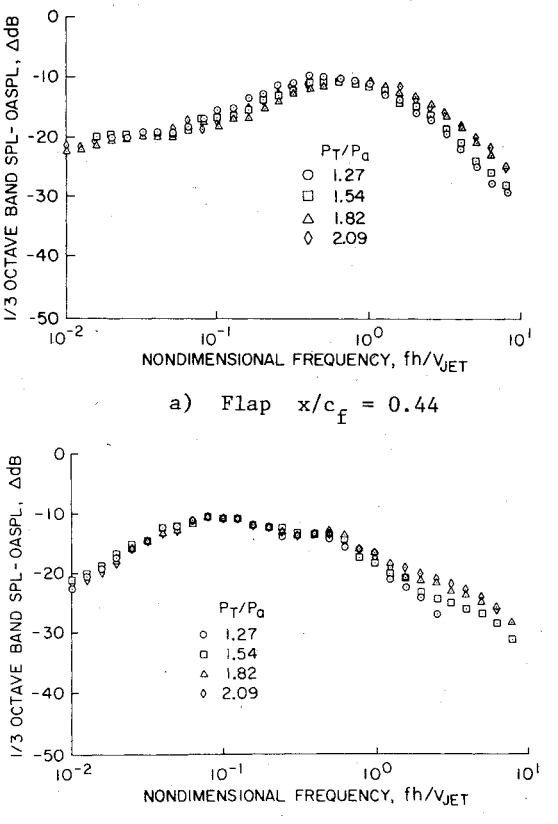

Fig. 6 Nondimensional surface pressure spectra.

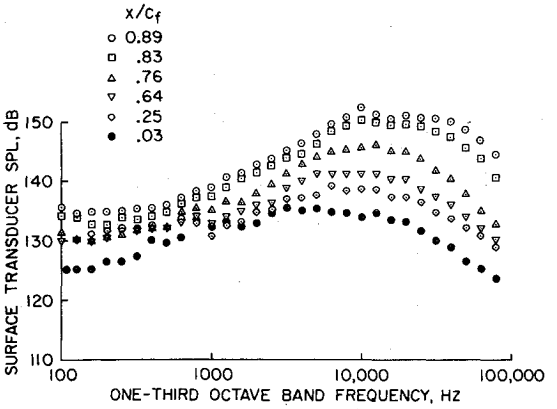

Fig. 7 Chordwise variation of flap surface pressure spectra; $P_T/P_a = 2.09$.

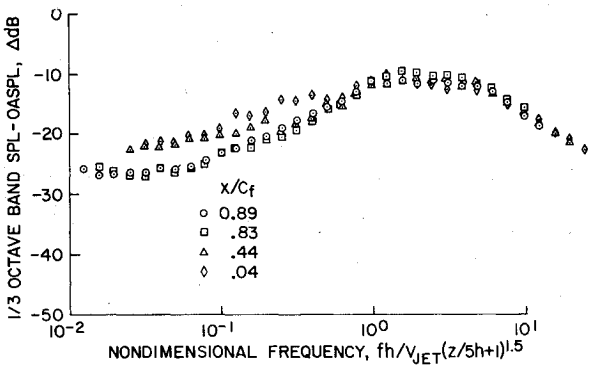

Fig. 8 Nondimensional chordwise variation of flap surface pressure spectra; $P_T/P_a = 2.09$.

nozzle height and primary nozzle velocity, and the SPL is normalized with respect to OASPL (see Fig. 6). This holds true only for cases where there is no screech interference.

As the distance from the nozzle increased, the intensity decreased, as did the peak frequency (see Fig. 7). Normalization of the chordwise variation is more difficult. It was shown by Maestrillo et al.[2] that the pressure in the near field of a three-dimensional jet can be normalized if the Strouhal number is modified by a factor $[(z/z_0) + 1]^3$, where $z_0 = 5$ (jet diameter). It was found in this case that substitution of the nozzle height for the jet diameter required that the factor exponent be replaced by 1.5 for the flap and by 4 for the shroud (see Fig. 8). This collapses the data on to a single curve, except at the low frequencies that exist as the trailing edge is approached.

A limited number of spanwise locations were measured near the flap leading and trailing edges. Near the flap leading edge, the individual lobes have not mixed completely, and each nozzle is still identifiable in the spanwise variation of surface pressure. As the flow progressed through the augmentor, the primary flow mixed with the entrained ambient air to become a single turbulent jet, showing a lack of significant spanwise variation in surface pressure.

Chordwise correlations were performed between pressure transducers to determine convective velocities in an attempt to identify acoustic and aerodynamic components. This was done for both the flap and shroud, and in each case the reference location was nearest the primary nozzle. Typical correlation coefficients in octave bands are shown in Fig. 9. The data show a sinusoidal oscillation at the frequency equal to the octave band center frequency, which decays in a $(\sin x)/x$ manner. The correlation coefficient can be used to determine the convective velocity by taking the delay time associated with the maxima of the cosine function envelope. Downstream, convective velocity was found to be 204 m/sec (670 fps) on the flap and 134 m/sec (440 fps) on the shroud.

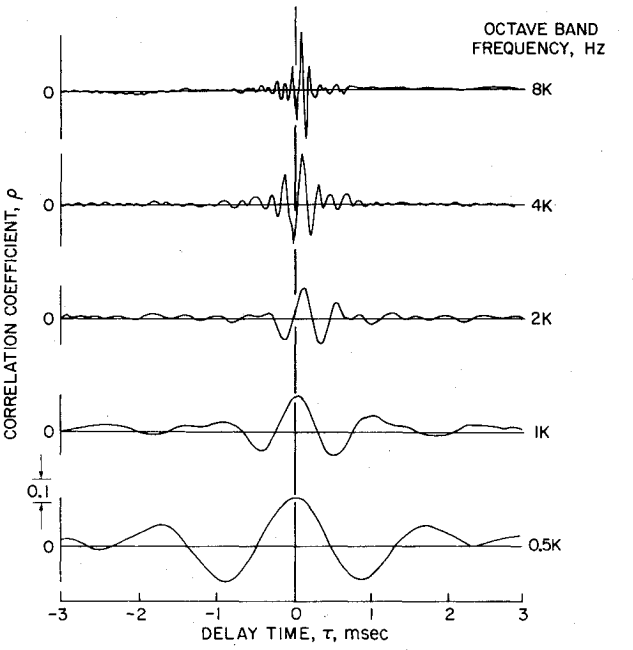

Fig. 9 Typical cross-correlation of surface pressure; $x/c_f = 0.89 \times 0.83$, $P_T/P_a = 2.09$.

Within experimental accuracy, the velocity was independent of a frequency range of 2000-8000 Hz. On the shroud, the 134-m/sec velocity was observed at $f = 1000$ Hz; no downstream convection was observed at this frequency on the flap. Data at 500 Hz were found to have no consistent trend. These results indicate that the main contributor to the surface pressure fluctuation was an aerodynamic pressure field that was convected downstream. The higher convective velocity on the flap might be expected from the augmentor exit velocity profiles. The flap convective velocity was approximately 0.6 V_{jet}, a value consistent with turbulent mixing results. If noise were being measured by the transducers, the convective velocity would have been equal to the local speed of sound plus the flow velocity.

Correlation of Far-Field Noise and Surface Pressures

Under ideal free-field conditions, the correlation coefficient relating surface and far-field pressure would show one maxima, at a time delay equal to the propagation time. However, in practice, other maxima may occur because of reflections and contributions from noise sources located away from the surface transducer. In this analysis, the propagation time was estimated, and the correlation maximum that occurred nearest this time was assumed to be associated with the direct path. No corrections have been applied to account for the presence of reflected or other signals; however, estimates indicate that such corrections would be small. Typical correlation data for each octave band frequency from 500 to 16,000 Hz are presented in Fig. 10. Further data for $f =$ 16,000 Hz are not shown because no significant correlation was observed. The chordwise variation of surface to far-field correlation for the flap and shroud is presented in Fig. 11. For both elements, the correlation decreased with increasing frequency, with the greatest decrease between 500 and 1000 Hz. The correlations associated with the trailing edge are similar for the flap and shroud. There is no consistency in the directivity of the trailing-edge correlation coefficient (see Fig. 12). The peak correlation occurs between 80°, depending on the frequency.

Effect of Forward Speed

For a jet, the peak radiated sound would be expected to decrease as the relative velocity decreased. On this basis, the

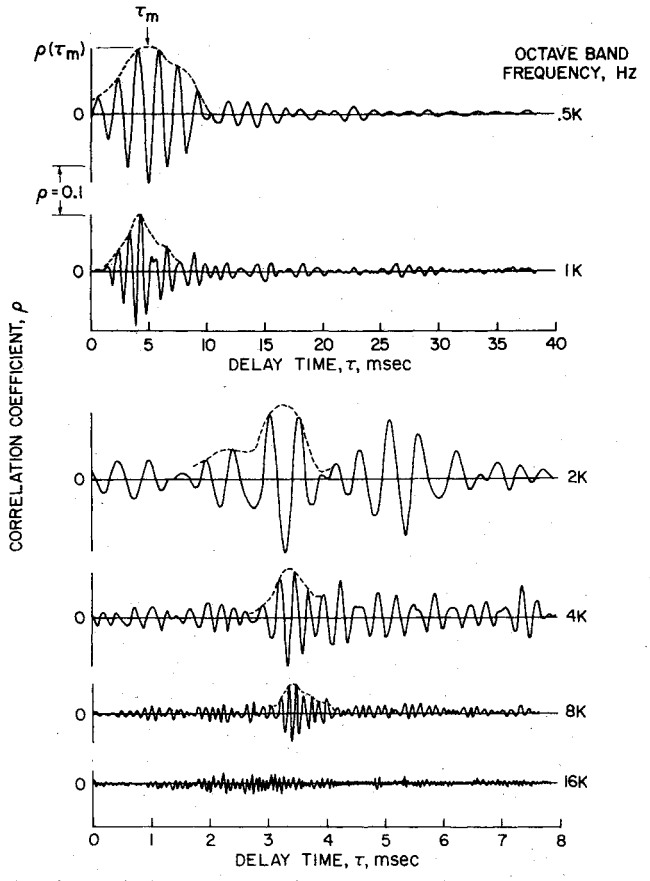

Fig. 10 Typical correlation of far-field noise with surface pressure; $\theta = 116°$, $x/c_f = 0.06$, $P_T/P_a = 2.09$.

expected reduction in acoustic power for $V_\infty = 49$ m/sec (160 fps) would be 4 dB. As has been shown before,[3] this was not the case for the augmentor; there was no consistent trend with forward speed. This was not the case for surface pressure characteristics. Near the trailing edges of the flap and shroud, the pressure levels below 1000 Hz decreased with forward speed (see Fig. 13). In addition, forward speed also reduced the surface far-field correlation even near the leading edge (see Fig. 14). The reduction of pressure and correlation is greatest and most consistent at 500 Hz.

Discussion

The principal objective of the present study was to examine the augmentor acoustic source characteristics, especially the source created by the flow turbulence interaction with the augmentor. This interaction with the internal surfaces will create what commonly is called scrubbing noise, and the flow past the augmentor exit will generate trailing-edge noise. Both of these acoustic sources have been shown to be significant in other powered-lift concepts.

Before drawing any conclusions regarding the noise sources of the augmentor, it is necessary to consider the role of the primary jet. Without the augmentor installed, the only source of noise will be created by the turbulent mixing of the primary jet and the ambient air. Many investigations have shown that the peak noise of a subsonic jet has an approximate V^8_{jet} dependence. Assuming that the nozzle width of 0.29 cm (0.115 in.) is the characteristic dimension and that the appropriate Strouhal number is 0.35, then for $V_{\text{jet}} = 335$ m/sec (1100 fps) the peak jet noise should be emitted at $f = 40{,}000$ Hz; this is coincident with the measured spectra peak (Fig. 6). The jet mixing noise from the individual lobe, therefore dominates the primary nozzle far-field noise. This conclusion is supported by the acoustic directivity results that are typical of jet mixing noise (Fig. 5).

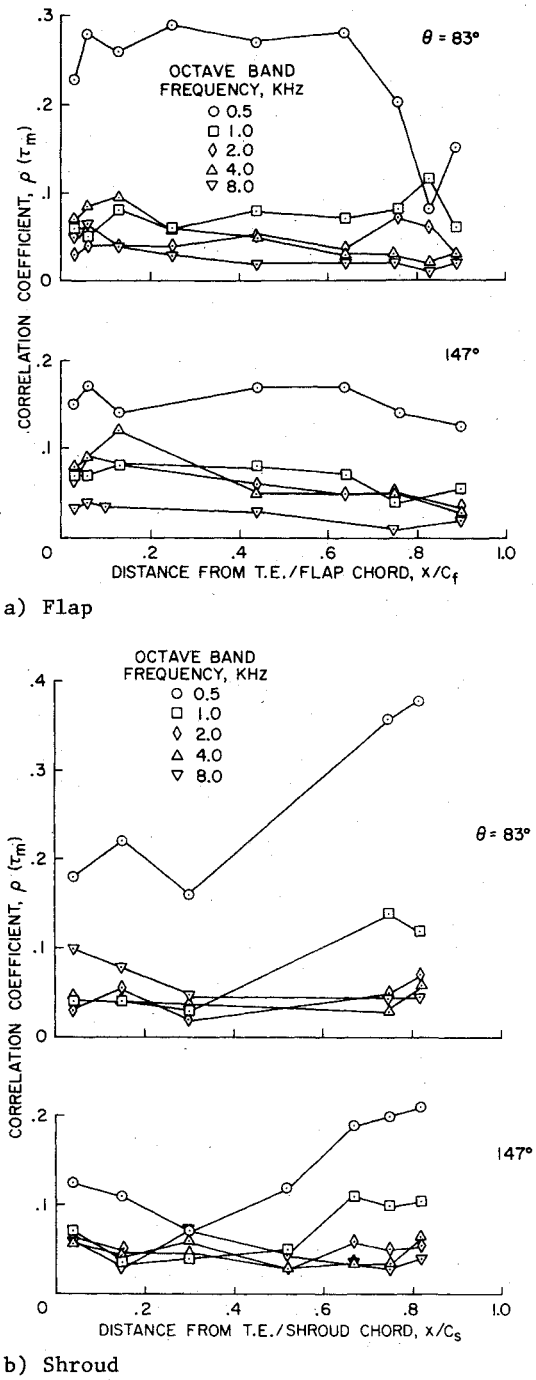

Fig. 11 Chordwise variation of surface to far-field correlations; $P_T/P_a = 2.09$.

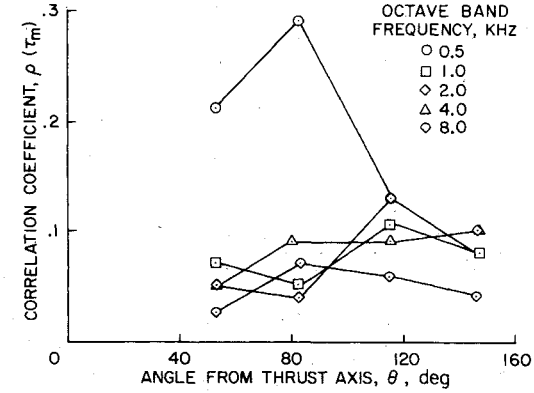

Fig. 12 Surface to far-field correlation directivity; $x/c_f = 0.04$, $P_T/P_a = 2.09$.

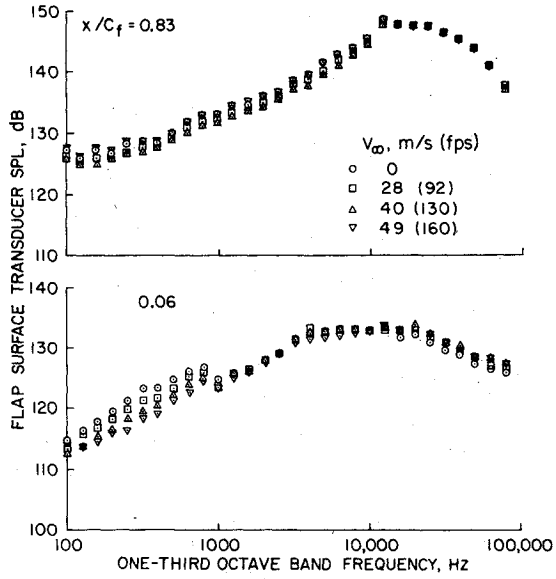

Fig. 13 Effect of freestream velocity on surface pressure; P_T/P_a = 2.09.

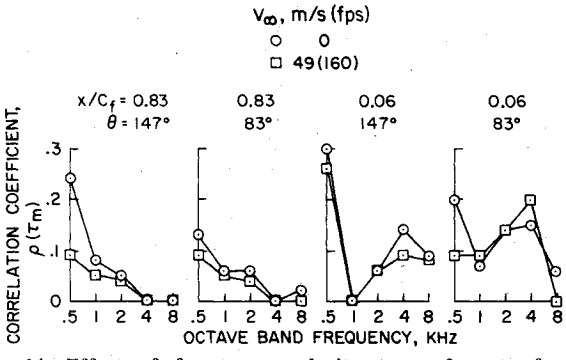

Fig. 14 Effect of freestream velocity on surface to far-field correlations; P_T/P_a = 2.09.

The augmentor modifies the primary jet-ambient air mixing process, as evidenced by the much increased air entrainment, which may in turn modify the jet noise sources. The augmentor also will modify the propagation to the far field of the jet noise created inside the augmentor. If it can be assumed that the axial source location is not affected by the augmentor, the source location can be estimated from MacGregor and Simcox.[4] The highest-frequency sources are located at the nozzle exit, with the source frequency decreasing with increasing axial distance from the jet exit. For the present study, the sources of f < 16,000 Hz are located from the nozzle exit to the augmentor inlet; sources of f = 2000 - 16,000 Hz are located inside the augmentor; and sources of f > 2000 Hz are located downstream of the augmentor exit. These source location estimates are supported by the results of the far-field acoustic measurements. The high-frequency noise generated near the nozzle would be emitted from the augmentor inlet and lower slot. As previously noted, this result was seen in the spectral directivity data. If the noise in the middle frequency range (2000 to 16,000 Hz is created inside the augmentor, the surfaces will prevent propagation to the far field until the noise reaches the augmentor exit. The augmentor exit plane then would seem to be the source of all of the internal jet noise. As noted previously, this characteristic also was evident in the directivity data.

Any dominant jet mixing sources that exist still should exhibit a V^8_{jet} dependency, even though generated internally. This eighth-power dependency could be seen in the noise with frequencies above 4000 Hz. The far-field acoustic characteristics, therefore, indicate that for this augmentor model the dominant acoustic mechanism is the jet mixing for f > 4000 Hz; this accounts for the low correlation of the surface pressure with far-field noise at 8000 Hz and the nonexistent correlation at high frequencies.

One anomaly remains in the acoustic results: although jet mixing sources normally are a function of relative velocity, such was not the case for the augmentor. The reason for this cannot be rationalized without further investigation of the influence of freestream velocity on the augmentor flow characteristics. It must be assumed that the acoustic sources associated with the dominant far-field noise are not affected to the first order by any change in the augmentor mixing process with airspeed.

Estimations of the location of the jet mixing noise source indicate that the low-frequency jet noise would be emitted downstream of the augmentor. The far-field noise measurement exhibits a V^5 to V^6 dependency, which is typical of dipole radiating acoustic sources, rather than the V^8 of turbulent mixing, as would be expected. The high surface pressure far-field corelations over this frequency range (f < 4000 Hz) show the flow turbulence interaction with the augmentor to be the significant contributor to the far-field noise. These correlations increase at the surface edges and are highest at 500 Hz, which is coincident with the peak in the noise spectra. The frequency of the peak trailing-edge noise can be estimated from the empirical technique described by Hayden,[5] which shows the Strouhal number for the spectral peak to be 0.04 to 0.06, where the characteristic dimension is defined as the distance from the edge to the maximum flow velocity. Using the augmentor exit flow results, the peak trailing-edge noise is estimated to occur at a frequency of 400 to 630 Hz, which again indicates that the low-frequency noise of the augmentor is dominated by flow turbulence interaction rather than jet mixing.

Significant surface to far-field correlations were measured along the augmentor surface as well as at the edges, indicating that surface interaction noise is also an important source of low-frequency noise. The correlation generally show this source to be less intense than the edge noise.

As was the case with the high-frequency jet noise, freestream velocity did not affect significantly, the far-field noise associated with the interaction of the flow turbulence with the augmentor. Although it did not affect the noise, forward speed did reduce the surface pressure levels and surface to far-field correlations, especially near the augmentor trailing edge. This would indicate that, although the trailing edge is a significant contributor to the far-field noise, it is not the dominant one. The surface interaction noise may be greater overall because of a greater number of sources, even though the correlations show lower values along the surface.

Concluding Remarks

As shown in previous studies, the overall noise of an untreated augmentor wing is dominated by the high-frequency jet mixing noise characteristic of the lobed primary nozzle. The augmentor modifies the intensity and propagation characteristics of the jet noise sources, especially those that exist inside the augmentor. This high-frequency jet mixing noise can be reduced by using an augmentor lining that is tuned to the mixing noise source location. If this is done, the low-frequency noise, which has been shown to be caused by the interaction of the flow turbulence with the augmentor, rather than turbulent mixing noise, probably will become an important noise source. This source, at least near the edges, appears to be affected favorably by forward speed.

References

[1] Campbell, J. M., Harkonen, D. L., and O'Keefe, J. V., "Design Integration and Noise Studies for Jet STOL Aircraft – Augmentor Wing Cruise Blowing Valveless System," NASA CR-114622, Vol. 1, Nov. 1973

[2]Maestrillo, L., Gedge, M. R., and Reddaway, A. R. F., "The Response of a Simple Panel to the Pseudo-sound Field of a Jet," *Aerodynamic Noise,* University of Toronto Press, Toronto, Ontario, Canada, 1969, pp. 189-208.

[3]Falarski, M. D., Aiken, T. N., Aoyagi, K., and Koenig, D. G., "Comparison of the Acoustic Characteristics of Large-Scale Models of Several Propulsive-Lift Concepts," *Journal of Aircraft,* Vol. 12, July 1975, pp. 600-604.

[4]MacGregor, G. R. and Simcox, C. D., "The Location of Acoustic Sources in Jet Flows by Means of the 'Wall Isolation' Technique," *AIAA Progress in Astronautics and Aeronautics: Aeroacoustics: Fan, STOL, and Boundary Layer Noise; Sonic Boom; Aeroacoustics Instrumentation,* Vol. 38, editor: Henry T. Nagamatsu; associate editors: Jack V. O'Keefe and Ira R. Schwartz, MIT Press, Cambridge, Mass., 1975, pp. 431-450.

[5]Hayden, R. E., "Noise from the Interaction of Flow with Rigid Surfaces," NASA CR-2126, April 1973.